

High-precision measurement of the thermal exponent for the three-dimensional XY universality class

Evgeni Burovski,¹ Jonathan Machta,¹ Nikolay Prokof'ev,^{1,2} and Boris Svistunov^{1,2}

¹*Department of Physics, University of Massachusetts, Amherst, Massachusetts 01003, USA*

²*Russian Research Center, "Kurchatov Institute," 123182 Moscow, Russia*

(Received 4 August 2006; published 3 October 2006)

Simulation results are reported for the critical point of the two-component ϕ^4 field theory. The correlation-length exponent is measured to high precision with the result $\nu=0.6717(3)$. This value is in agreement with recent simulation results [Camprostrini *et al.*, Phys. Rev. B **63**, 214503 (2001)] and marginally agrees with the most recent space-based measurements of the superfluid transition in ^4He [Lipa *et al.*, Phys. Rev. B **68**, 174518 (2003)].

DOI: 10.1103/PhysRevB.74.132502

PACS number(s): 64.60.Fr, 05.10.Ln, 67.40.-w

Universality at critical points is among the most beautiful and powerful ideas to emerge from statistical physics.¹ The universality hypothesis asserts that critical exponents and some other asymptotic properties of critical points are independent of microscopic details and depend on only a few properties such as the symmetry of the order parameter and spatial dimensionality. Universality permits the calculation of critical exponents for experimental systems using simplified and optimized model systems with the same symmetries. The theory of critical phenomena also predicts relationships among critical exponents. Among these relations are the hyperscaling relation $\alpha=2-d\nu$ between the specific-heat exponent α , the correlation-length exponent ν , and the dimensionality d and the Josephson relation $\zeta=(d-2)\nu$ for the superfluid-stiffness exponent ζ . Improvements in experiments, theory, and computer simulations have led to increasingly strict tests of universality and scaling relations. By far the most accurate experimental measurements of critical exponents are for the superfluid transition in ^4He , which is in the $O(2)$ or XY universality class. The purity of liquid helium together with the stability of temperature control and the accuracy of specific-heat measurements at low temperatures means that the limiting factor in approaching the critical singularities is the rounding due to the Earth's gravitational field.² To overcome gravitational rounding, space-based microgravity experiments have been devised³ that achieve four-significant-digit accuracy for the specific-heat exponent α . These experimental results seemingly do not agree with either analytical or numerical calculations. The experimental value itself has evolved with time due to the reanalysis of the data (see Refs. 3–5), the most recent reported value being $\nu_{\text{exp}}=0.6709(1)$, as inferred from the measured value of α via the hyperscaling relation.

A number of recent analytical and numerical calculations were aimed at high-precision determinations of ν for the XY universality class. The vortex-loop calculations by Williams⁶ yield $\nu=0.6717$. Török and Hasenbusch⁸ studied the two-component ϕ^4 model via Monte Carlo simulations. This model has a parameter that adjusts the softness of the potential-constraining-amplitude fluctuations of the order parameter. These authors took advantage of this freedom to suppress the leading corrections to scaling. This study resulted in $\nu=0.6723(3)(8)$ (the statistical and systematic er-

rors are given in the first and second parentheses, respectively). Later the effort was advanced by Camprostrini *et al.*⁷ who combined Monte Carlo simulations with a high-temperature expansion to obtain $\nu=0.67155(27)$, which agrees with the experimental result at the level of two standard deviations. Our study also employs a ϕ^4 model with fine tuning of the Hamiltonian.

Purely analytic studies of the XY critical point include extensive treatments by Guida and Zinn-Justin, summarized in Ref. 9, which yield $\nu=0.6703(15)$ for the perturbative seven-loop expansion in $d=3$, and $\nu=0.6680(35)$ for the ϵ expansion up to the order ϵ^5 . Jasch and Kleinert¹⁰ developed a Borel resummation technique in the context of a strong-coupling theory which results in $\nu=0.6704(7)$. The history of recent results for the correlation-length exponent is given in Fig. 1.

The purpose of this paper is to provide high-precision-simulation results for the exponent ν for the three-dimensional (3D) XY universality class using only the Monte Carlo simulations and to compare with other theoretical, computational, and experimental results.

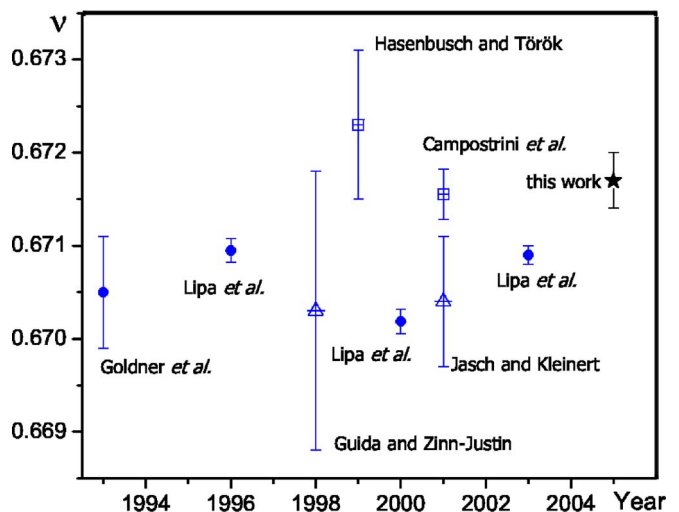


FIG. 1. (Color online) Results for ν as a function of time. Filled circles show the experimental values, open triangles depict the field-theoretic calculations, and squares show the Monte Carlo results.

We study a discrete 3D classical ϕ^4 model defined by the Hamiltonian

$$\frac{H}{T} = -t \sum_{\langle ij \rangle} \phi_i^* \phi_j + (U/2) \sum_i |\phi_i|^4 - \mu \sum_i |\phi_i|^2, \quad (1)$$

where i and j label the sites of a simple 3D cubic lattice with periodic boundary conditions; $\langle ij \rangle$ stands for the pairs of nearest-neighbor sites and ϕ_i is the complex order parameter field. Since ϕ_i fields are continuous and unbounded, the model (1) has only two independent parameters: by rescaling fields one can always set one parameter to unity. Henceforth we set $\mu=1$.

In order to simulate the model (1), we employ the high-temperature expansion for the partition function, which transforms the configuration space into that of closed oriented loops. The latter can be efficiently sampled by the worm algorithm,¹¹ which switches between the partition function and Green-function sectors. The worm algorithm has virtually no critical slowing down and provides a direct access to the statistics of winding-number fluctuations, which, in turn, define the superfluid stiffness¹²

$$\rho_s L = \sum_{a=1}^d \langle W_a^2 \rangle / 2d. \quad (2)$$

Here L is the linear system size, W_a is the winding number in the a th direction, and angular brackets denote averaging over the Gibbs distribution. One can also devise direct Monte Carlo estimators for the derivatives of ρ_s with respect to t and/or U , which involve cross correlations between energy and winding numbers.

In the renormalization-group (RG) framework, the finite-size scaling of the superfluid stiffness obeys the relation

$$\rho_s L = f(x) + g_\omega(x) y_\omega L^{-\omega} + \dots, \quad (3)$$

where $x=(L/\xi)^{1/\nu}$ is the dimensionless scaling variable, $\xi=\xi(t, U)$ is the correlation length, $f(x)$ and $g(x)$ are universal functions that are analytic as $x \rightarrow 0$, y_ω is the leading irrelevant scaling field, and the ellipsis represents the higher-order corrections. Field-theoretical calculations⁸ yield $\omega=0.802(11)$ (ϵ expansion) and $\omega=0.789(11)$ ($d=3$ loop expansion), and the numerical analysis of Ref. 7 gives $\omega=0.795(9)$.

By differentiating Eq. (3) with respect to t for $U=U_c$ and then letting $t \rightarrow t_c$, one transforms Eq. (3) into

$$R'_c = AL^{1/\nu}(1 + CL^{-\omega}) + \text{higher-order terms}. \quad (4)$$

Here the derivative of $R \equiv \rho_s L$ is taken at the critical point, and A and C are nonuniversal constants. Equation (4) is especially convenient for the numerical data analysis: the log-log plot of R'_c versus L is a straight line with the slope $1/\nu$ for sufficiently large L . The second term adds a slight concavity or convexity to the curve for intermediate system sizes, depending on the sign of C . It is argued in Refs. 6 and 7 that there is little advantage in using improved models if corrections to scaling are included in the fits of MC data and two alternative strategies of dealing with the problem are suggested. One is that MC data are fitted by discarding

TABLE I. Results for critical points \mathcal{A} and \mathcal{B} .

L	R'_A	R'_B
4	2.0329(9)	1.9906(3)
5	2.8414(5)	2.7842(7)
6	3.7316(4)	3.6583(9)
7	4.6955(5)	4.6060(5)
8	5.7289(4)	5.6215(9)
9	6.8265(7)	
10	7.9848(9)	7.839(1)
11	9.2031(13)	
12	10.474(2)	10.284(1)
16	16.074(4)	15.784(2)
20	22.403(4)	22.011(3)
24	29.396(7)	28.883(3)
32	45.095(13)	44.33(1)
48	82.48(3)	81.05(2)
64		124.40(4)
96	231.56(17)	

correction-to-scaling terms, and the possible systematic error thus introduced is estimated from the universal amplitude ratios. The other is that MC data for the critical point are used in the analysis of the high-temperature expansion series. We demonstrate below that comparable accuracy can be achieved by Monte Carlo simulations alone, using joint fits of several improved models.

In order to locate a particular critical point, we fix some value of t and then plot $R = \rho_s L$ as a function of U for different system sizes. The crossing of these curves in the limit of $L \rightarrow \infty$ gives the critical point.¹³

We first consider the critical point $t_A = -0.079\,554\,8$ and $U_A = 0.410\,156\,2(14)$, which we denote by \mathcal{A} . This critical point was previously studied by Campostrini *et al.*⁷ who performed an extensive and thorough search of improved models.¹⁷

The accuracy of the critical-point determination is verified by an independent Monte Carlo measurement of the first and second derivatives of R . Indeed, suppose that for a given $U=U_c$ the value of t is off by $\delta t = t - t_c$. Then, expanding Eq. (3) up to $O(\delta t^2)$ and using the data from Table I, one makes sure that (i) the deviations of R_c from its universal value 0.2580(3) are consistent with $\delta t \sim 10^{-6}$, and (ii) the $O(\delta t^2)$ terms are smaller than statistical errors and thus can be safely neglected. For example, $R_A(L=48) = 0.2583(1)$ and $R''_A(L=48) = 2.65 \times 10^4$. The derivatives for $L \neq 48$ can be computed using $R' \propto L^{1/\nu}$ and $R'' \propto L^{2/\nu}$ [cf. Eq. (3)].

Table I lists the raw data for $\rho'_s L$ (see below for the discussion of the data set \mathcal{B}). Each data point was obtained from not less than 5×10^8 sweeps (upon equilibrating) and the accumulated data set represents approximately 18 years of CPU time. Error bars are one standard deviation and were obtained using the blocking method.

In order to magnify the fine details, we scale the numerical data with the experimental exponent

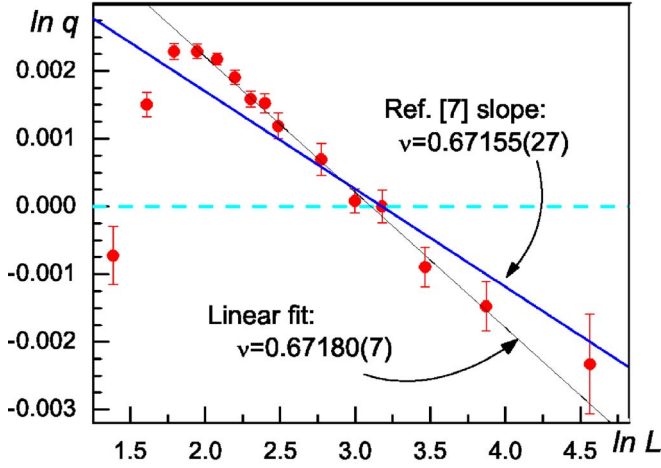


FIG. 2. (Color online) The derivative of $R_{\mathcal{A}}$ rescaled via Eq. (5). The dashed horizontal line corresponds to $\nu = \nu_{\text{exp}}$. (See the text for a discussion.)

$$q(L) = \frac{R'_c(L)L^{-1/\nu_{\text{exp}}}}{R'_c(L_0)L_0^{-1/\nu_{\text{exp}}}} \quad (5)$$

and normalize it at an arbitrarily chosen value $L_0=24$. Figure 2 shows the data for critical point \mathcal{A} , rescaled using Eq. (5). Given the error bars, it appears that corrections to scaling are relevant only for $L \leq 10$ and for $L \geq 10$ a straight line with the slope equal to $1/\nu - 1/\nu_{\text{exp}}$ is a good fit [see Eqs. (4) and (5)]. A linear fit of the data for $L \geq 10$ yields $\nu_{\mathcal{A}}=0.67180(7)$ in a flagrant disagreement with the experimental value $\nu_{\text{exp}}=0.6709(1)$. Our value $\nu_{\mathcal{A}}$ is in agreement with the value $\nu=0.67155(27)$ of Ref. 7 within the combined error bars. However, our new data for the critical point \mathcal{A} are more accurate and yield a smaller error bar.

We have also studied a version of the improved link-current model,¹⁵ which belongs to the same universality class. When these data were fit by a straight line, we observed even greater discrepancies with ν_{exp} .

To understand the apparent disagreement with experiment, we performed a series of simulations for critical points in the vicinity of the critical point \mathcal{A} to map out the region where $C=C(t_c, U_c)$ is small. We then carried out a large-scale simulation of one of the critical points \mathcal{B} characterized by $t_{\mathcal{B}}=-0.07142822$ and $U_{\mathcal{B}}=0.3605750(8)$. Table I shows the raw data for this critical point [$R_{\mathcal{B}}(L=48)=0.2577(1)$ and $R''_{\mathcal{B}}(L=48)=1.27 \times 10^4$]. A naïve linear fit of the data set \mathcal{B} for $L \geq 10$ yields $\nu_{\mathcal{B}}=0.67142(5)$, which is inconsistent with $\nu_{\mathcal{A}}$. Critical points \mathcal{A} and \mathcal{B} are equally legitimate and we are left in a quandary as to whether to reject universality or to consider a more careful analysis of the data. We choose the latter course.

It becomes obvious that there is no easy way to improve the accuracy of the critical-exponent calculations by ignoring corrections to scaling, even when they appear very small. To reconcile the results for the data sets \mathcal{A} and \mathcal{B} one *must* include the subleading corrections in the fits. If this is done for each data set separately, it leads to a large increase (almost by an order of magnitude) in the uncertainty of the fits,

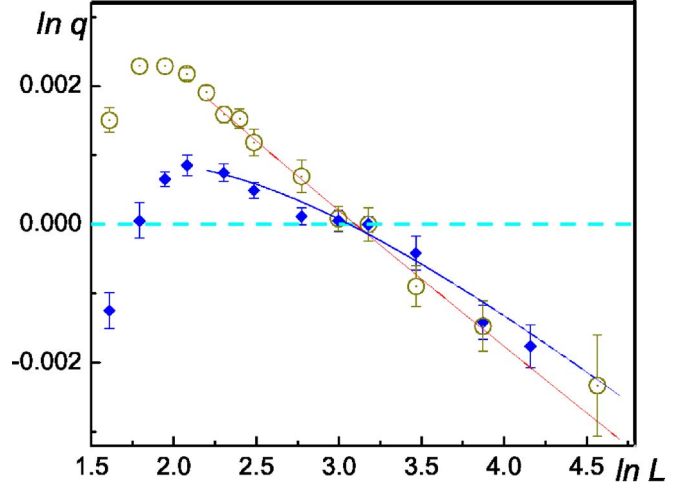


FIG. 3. (Color online) Data from Table I rescaled via Eq. (5). Circles: data set \mathcal{A} ; diamonds: data set \mathcal{B} . The dashed horizontal line corresponds to $\nu = \nu_{\text{exp}}$. The solid lines are the results of the joint fit of both data sets. (See the text for an explanation.) Note the scale of the vertical axis.

as has been noted in Ref. 7. Tighter error bars can be obtained performing a *joint* fit of two data sets. More specifically, we perform a six-parameter fit according to

$$\ln q \sim B + \left(\frac{1}{\nu} - \frac{1}{\nu_{\text{exp}}} \right) \ln(L/L_0) + CL^{-\omega}, \quad (6)$$

as follows from Eqs. (4) and (5) for $C \ll 1$. The fitting parameter B is introduced in order to undo the artificial normalization $q(L=L_0)=1$. Here each critical point has its own amplitudes B and C , while the universal exponents ν and ω are shared between the data sets, which yield six fitting parameters.

We performed the joint fit according to Eq. (6) via the stochastic minimization of χ -square. We constrained the exponent ω to within ± 0.03 around 0.795, which is the 3σ interval of the established value.⁷ We also discarded small system sizes $L < L_{\text{cutoff}}=10$. The optimization procedure yields $\nu=0.6717(3)$ at the confidence level¹⁴ (CL) ≈ 0.43 . This value is consistent with the result of Ref. 7 and also marginally agrees with the experimental value of Ref. 3. The fit is depicted in Fig. 3 and yields

$$C_{\mathcal{A}} = (1.5 \pm 0.5) \times 10^{-3},$$

$$C_{\mathcal{B}} = (-1.0 \pm 0.3) \times 10^{-2},$$

$$\nu = 0.6717(3). \quad (7)$$

Note that the data-set \mathcal{A} points are exactly the same as in Fig. 2 and a slight curvature is visible in Fig. 3 which is unaccounted for in Fig. 2. It is also worth noting that the best-fit value of ω is $\omega=0.81(1)$, which is consistent with the

field-theoretic estimates.⁸ The error bars in Eq. (7) reflect both stochastic and systematic uncertainties, the latter being estimated via changing the L_{cutoff} for the data set \mathcal{A} and/or \mathcal{B} .

One might question the relevance of higher-order corrections to scaling omitted from Eq. (3). The next-order correction is proportional to the square of the leading irrelevant field $\propto C^2 L^{-2\omega}$, i.e., it contains the square of the already small amplitude C .¹⁶ A sizable cumulative amplitude of higher-order corrections would exhibit itself for the smallest system sizes $L \lesssim 12$. On the contrary, the scaling curves for both models under consideration have an overall vertical scale on the order of 10^{-3} for system sizes as small as $L=4$.

Our calculated value of $\nu=0.6717(3)$ is in agreement with the results of recent simulation⁷ and also marginally agrees

with the best experimental value $\nu_{\text{exp}}=0.6709(1)$, deduced from α via hyperscaling relation. We demonstrate that one has to be careful when working with improved models and always include corrections to scaling into the fit, even when the data set allows a good linear fit. Four-digit accuracy in critical exponents is reached by simultaneously fitting more than one critical point.

Noted added in proof. Recently, Campostrini *et al.* communicated the result $\nu=0.6717(1)$ (Ref. 18), which confirms all four significant digits of our value of ν and has even smaller errorbar.

We acknowledge support from NASA under Grant No. NAG-32870.

¹M. E. Fisher, in *Critical Phenomena*, Lecture Notes in Physics Vol. 186 (Springer-Verlag, Berlin, 1983).

²L. S. Goldner, N. Mulders, and G. Ahlers, *J. Low Temp. Phys.* **93**, 131 (1993).

³J. A. Lipa, J. A. Nissen, D. A. Stricker, D. R. Swanson, and T. C. P. Chui, *Phys. Rev. B* **68**, 174518 (2003).

⁴J. A. Lipa, D. R. Swanson, J. A. Nissen, Z. K. Geng, P. R. Williamson, D. A. Stricker, T. C. P. Chui, U. E. Israelsson, and M. Larson, *Phys. Rev. Lett.* **84**, 4894 (2000).

⁵J. A. Lipa, D. R. Swanson, J. A. Nissen, T. C. P. Chui, and U. E. Israelsson, *Phys. Rev. Lett.* **76**, 944 (1996).

⁶G. A. Williams, *Phys. Rev. Lett.* **82**, 1201 (1999).

⁷M. Campostrini, M. Hasenbusch, A. Pelissetto, P. Rossi, and E. Vicari, *Phys. Rev. B* **63**, 214503 (2001).

⁸M. Hasenbusch and T. Török, *J. Phys. A* **32**, 6361 (1999).

⁹R. Guida and J. Zinn-Justin, *J. Phys. A* **31**, 8103 (1998).

¹⁰F. Jasch and H. Kleinert, *J. Math. Phys.* **42**, 52 (2001).

¹¹N. Prokof'ev and B. Svistunov, *Phys. Rev. Lett.* **87**, 160601 (2001).

¹²E. L. Pollock and D. M. Ceperley, *Phys. Rev. B* **36**, 8343 (1987).

¹³K. Binder, *Phys. Rev. Lett.* **47**, 693 (1981).

¹⁴W. H. Press, S. A. Teukolsky, W. T. Vetterling, and B. P. Flannery, *Numerical Recipes in C*, 2nd edition (Cambridge University, Cambridge, England, 1992).

¹⁵M. Wallin, E. S. Sørensen, S. M. Girvin, and A. P. Young, *Phys. Rev. B* **49**, 12115 (1994).

¹⁶M. Hasenbusch, *J. Phys. A* **32**, 4851 (1999).

¹⁷The notation of Ref. 7 is related to ours via $t=\beta/2(2\lambda-1)$ and $U=2\lambda/(2\lambda-1)$.

¹⁸M. Campostrini, M. Hasenbusch, A. Pelissetto, and E. Vicari, cond-mat/0605083.